Tunable fiber ring laser with an intracavity high resolution filter employing two-dimensional dispersion and LCoS modulator

David Sinefeld* and Dan M. Marom

Applied Physics Department, Hebrew University, Jerusalem 91904, Israel
**Corresponding author: sinefeld@gmail.com*

Received September 15, 2011; revised November 10, 2011; accepted November 10, 2011;
posted November 10, 2011 (Doc. ID 154804); published December 16, 2011

We demonstrate a tunable fiber ring laser employing a two-dimensional dispersion arrangement filter, with the lasing determined by a liquid crystal on silicon (LCoS) spatial light modulator. Lasing wavelengths can be tuned discontinuously across the communication *C*-band at an addressable resolution of less than 200 MHz. We introduce full characterization of the laser output including phase and amplitude stability and short and long-term bandwidth measurements. © 2011 Optical Society of America

OCIS codes: 060.2330, 060.2320, 140.3510.

Tunable fiber ring lasers have important applications in optical communication systems, fiber sensors, infrared spectroscopy, and optical instrumentation, as they offer easy integration with these all-fiber systems [1–4]. Lasing wavelength tuning is achieved by a filter placed inside the ring cavity, where the tuning mechanism can be based on a Fabry–Perot etalon [5,6], a fiber Bragg grating [7,8], or electro-optic [9], piezo-electric [10], and acousto-optic [11] modulators. A gain element (typically a fiber amplifier) and an output coupler complete the ring cavity (see the inset of Fig. 1). These lasers are favorably characterized by a high side mode suppression ratio (SMSR) and a large tuning range, but their tuning is continuous along the spectrum due to the filter characteristics, which is not acceptable in certain applications such as optical communications. This can be alleviated by extra hardware to prevent laser output during tuning events, impacting cost.

In the last couple of years, tunable fiber lasers based on an intracavity, free-space, adaptive filter employing a spatial light modulator (SLM) and a diffraction grating were introduced [12–13]. This arrangement allows full access to all the spectral components and enables discontinuous lasing wavelength jumps. However, the tuning performances of the reported fiber lasers were limited due to the relatively low resolution and addressability of the filter's diffraction grating and SLM. We recently presented [14] a tunable fiber ring laser employing an extremely high resolution filter utilizing a two-dimensional (2D) dispersion arrangement [15]. With this combination, we have demonstrated a tunable ring laser with a tuning resolution of 200 MHz along 30 nm (the communication *C*-band). This paper provides further design details and full characterization of our 2D tunable fiber laser.

The layout and concept of the 2D filter arrangement is shown in Fig. 1 and discussed in detail in [15]. Light is angularly dispersed using a 2D optical arrangement from two crossed gratings: a high resolution waveguide grating router (WGR) and a free-space bulk grating. The 2D dispersed light is projected with a Fourier lens onto a liquid crystal on silicon (LCoS), 2D, pixelated, phase-only modulator. The WGR has a free spectral range (FSR) of 100 GHz and a spectral resolution of 3 GHz. The crossed 1200 gr/mm holographic diffraction grating placed after the WGR separates the diffraction orders in the orthogonal direction. The resultant dispersion forms a contiguous series of dispersed 100 GHz channels on the spectral plane (Fig. 2(a)). At this plane, we place the LCoS reflective modulator with 512×512 square pixels of 15 μm pitch (total size of 7.68×7.68 mm^2), capable of prescribing phase delays $\in [0, 2\pi]$. The spatial dispersion in the WGR direction results in 512 columns spanning a 93 GHz wide spectrum. Each column of the modulator addresses a particular center frequency, at 182 MHz shift in center frequency. The spatial dispersion in the bulk grating direction results in an offset of 15 pixels for successive diffraction orders (spaced at 100 GHz). Because of the limited size of our LCoS SLM, only 30 WDM channels spaced at 100 GHz are modulated and reflected back. We set the lasing wavelength by attenuating all wavelengths (by setting a linear phase ramp that reduces the coupling back), except for the particular wavelength that is transmitted, seen as a clear window with no phase tilt applied (see Fig. 2(b)).

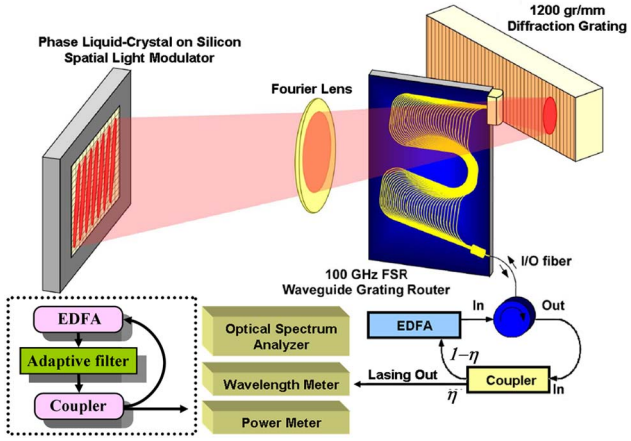

Fig. 1. (Color online) Layout of the ring laser: amplified light goes through crossed gratings (waveguide grating router (WGR) and bulk), which disperse the spectrum across the two-dimensional LCoS array, enabling high resolution access to the spectral components along the communication *c*-band. Inset: layout of a ring laser based on an adaptive filter and gain module inside the cavity.

The window spans 18 pixels along the high dispersion axis, matching the optical resolution (setting it smaller only increases the loss). The ring cavity is completed with a circulator (couple in and out of our filter), an erbium doped fiber amplifier (EDFA), and an output coupler. The first lasing experiment used a 90/10 output coupler (10% output) placed after the EDFA, and lasing was observed on an optical spectrum analyzer (OSA). Changing the horizontal position of the window results in jumping from one diffraction order to another, leading to a 100 GHz change in the output wavelength (Fig. 3(a)). Changing the vertical position of the window, along a specific diffraction order, results in fine changes in the output wavelength with a spectral step size of l82 MHz (Fig. 3(b)). We coarsely tune the wavelength by selecting the WGR diffraction order (separated by the bulk grating) and finely tune the wavelength by selecting within the WGR diffraction order. The insertion loss of the 2D filter arrangement is approximately 14 dB (mostly due to coupling from the planar light circuit (PLC)); hence we use an EDFA amplifier with 22 dB gain and 18 dBm saturation power. This leads to a gain saturated output power level of 8 dBm (using the 10% tap, i.e., 10 dB less that the EDFA saturation power), constant along the output spectrum (Fig. 3). The SMSR is greater than 50 dB.

We experimented with different output coupler values and positions, using three available couplers with splitting values of 1/99, 10/90, and 50/50, providing five output coupling values: 1%, 10%, 50%, 90%, and 99%. We also swapped the position of the EDFA and the tap splitter. In each of the above arrangements, we measured both the output power and the SMSR (see Fig. 4). The highest output power was measured with the 50% output tap with the EDFA before the tap splitter, resulting in 15 dBm output power (3 dB less than the EDFA saturation level due to the 50/50 output coupler). For 1% output, we measured output of −2 dBm, e.g., 20 dB less than the saturation level. Those three results imply that the EDFA reached its saturation level. However, when we used an output coupler of 90% and 99%, the losses of the ring cavity were too high, the EDFA was unsaturated, and the laser output power was lower. In the case of EDFA after

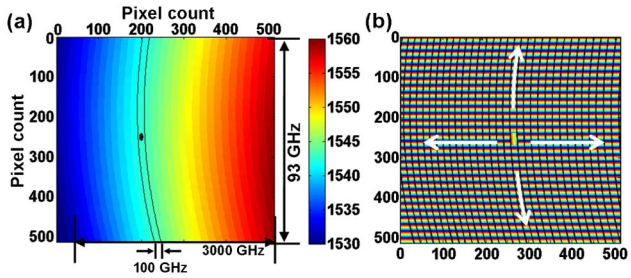

Fig. 2. (Color online) (a) 2D spatial wavelength dispersion on the SLM. The WGR provides high resolution on the narrow FSR. The bulk grating separates the WGR diffraction orders. The black lines mark the borders of a specific WGR diffraction order, while the black ellipse denotes the spot size for a specific wavelength. (b) Exemplary applied LCoS phase, attenuating all spectral components except the lasing line, which appears as an open window. Scanning the lasing window along the white arrows selects the lasing frequency (horizontal translation selects WGR diffraction order; vertical translation selects along the fast axis or within the diffraction order).

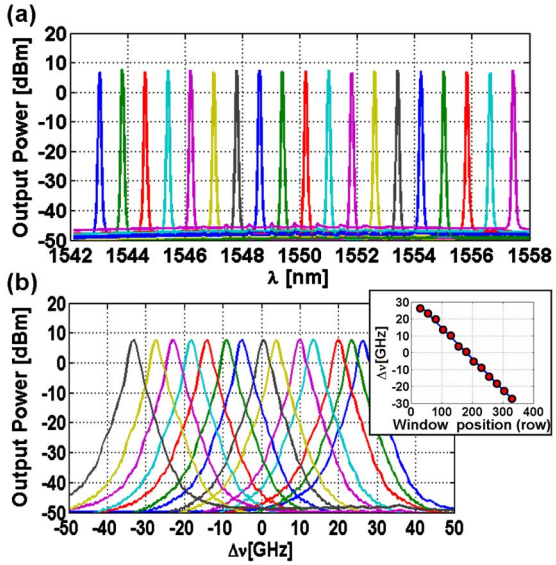

Fig. 3. (Color online) Output of the fiber laser. (a) Laser lines from different diffraction orders of the WGR. (b) Laser lines from different locations of the same WGR diffraction order. Inset: linear fit of the center frequency verses mask opened window position, resulting in a slope of 182 MHz per SLM row. The slight deviation from linearity is caused by the uncertainty in the lasing line position within the 3 GHz spectral window.

the coupler, we have the same curve shape but with much lower output power due to the filter's 14 dB attenuation. The SMSR depends on the EDFA location too, where in the case of EDFA after coupler, better results are obtained (except for the extreme cases of the 1/99 coupler, in which the output power is lower than −20 dBm and the SMSR is therefore lower). The best performance was obtained when the EDFA was placed before a 10% coupler output resulting in 8 dBm output power and an SMSR of 58 dB.

The spectral plots of the laser output, as shown in Fig. 3(b), do not reflect the actual laser line width, but rather reflect the OSA resolution limit. To properly measure the laser line width, we mixed our fiber laser output with that of a reference 100 KHz line width external cavity laser. The reference laser was set to a slightly different wavelength, resulting in an intermediate frequency beating between the two lasers. This was detected with a high speed photodetector connected to a high speed real-time scope (Fig. 5(a)). In adddition, a slow detector was connected directly to the fiber laser to track its output

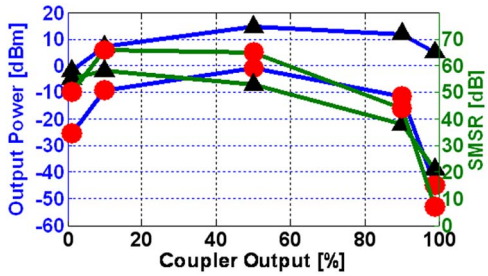

Fig. 4. (Color online) Output power (blue line) and SMSR (green line) of the fiber laser versus output tap value, measured in various combinations: (a) EDFA before the coupler (results marked with black triangles); (b) EDFA after the coupler (results marked with red circles).

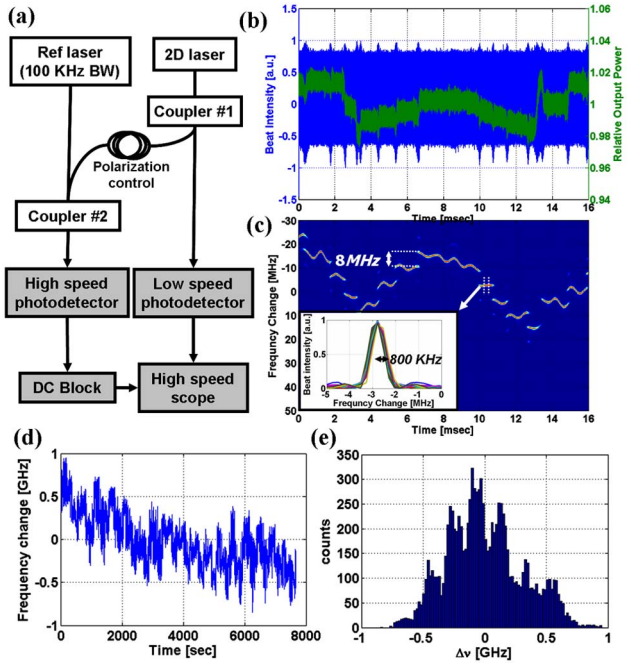

Fig. 5. (Color online) Measuring laser line width. (a) Setup for line width measurement using a high speed detector to measure the beating between a reference laser and the 2D laser, while a slow detector measures the direct output power of the 2D laser. (b) Registered powers of the beat frequency (blue) and the output power (green), with correlation between intensity spikes and mode hops. (c) Spectrogram of the interferometric measurement showing mode hops occurring every 1-3 ms. Frequency hop is approximately 8 MHz. Inset: cross section of the spectrogram showing instantaneous laser line width of 800 KHz. (d) Results of 10 000 measurements of laser relative lasing frequency taken along 8000 seconds. The central frequency changes are due to mode hoping and thermal drift. (e) Histogram of the above 10 000 measurements showing the long-term frequency excursion of the laser output.

power. The detected power results are shown in Fig. 5(b). Changes in the relative frequency between the 2D and the reference laser are shown as "spikes" in the beat intensity, and they correlate with power changes with a transient duration of a few microseconds. A spectrogram of the beat intensity measurement (Fig. 5(c)) shows that every few milliseconds a mode hopping event occurs inside the ring laser, with a lasing frequency hop of approximately 8 MHz. This correlates to a fiber cavity length of 38 meters, which is reasonable due to the EDFA fiber length. A vertical cross section of the spectrogram (shown in the inset of Fig. 5(c)) shows the instantaneous laser line width is approximately 800 KHz. This narrow line width can be utilized in self-homodyne sensing applications. However, the rapid mode hopping likely precludes the laser's use in other coherent reception applications, and in application requiring high intensity stability. A histogram of 10 000 relative frequency measurements taken with an ~1 second interval in an uncontrolled environment gives the long duration lasing wavelength stability bandwidth of 1.3 GHz (Fig. 5(d)–(e)). This bandwidth is smaller than the 3 GHz filter window, since the lasing preferentially occurs close to the filter peak, where losses are minimal. In order to examine the output power stability of the laser, an intensity measurement was performed over 800 seconds

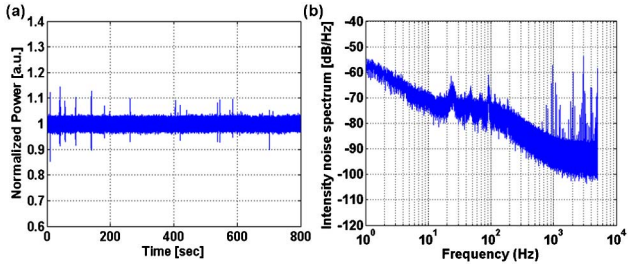

Fig. 6. (Color online) Laser output power measurements: (a) Intensity measurement versus time taken over 800 seconds sampled at 10 KHz. (b) RIN measurement results.

(Fig. 6(a)), resulting in a small change in output power along the measurement. The power spectrum of this measurement, shown in Fig. 6(b), expresses the relative intensity noise (RIN) of the laser output. The spikes shown in the RIN plot around 1 KHz are attributed to the mode hoping rate, which is accompanied by intensity changes every few milliseconds.

In summary, we demonstrated the functionality of a tunable ring laser based on a high resolution, 2D dispersive arrangement and an EDFA gain amplifier. We operated the laser with various coupler ratios and EDFA positions and found a configuration that gave maximal output power of 15 dBm and SMSR greater than 50 dB with a tuning ability of less than 200 MHz along the *C*-band. We have measured the spectral bandwidth of the laser, resulting in a long duration bandwidth of 1.3 GHz and an instantaneous bandwidth of 800 KHz and output power stability of a few percent.

References

1. L. Paraschis, O. Gerstel, and R. Ramaswami, in *Proceedings of Optical Fiber Communication Conference* (Optical Society of America, 2004), Paper MF105.
2. N. J. C. Libatique and R. K. Jain, IEEE Photon. Technol. Lett. **13**, 1283 (2001).
3. K. T. V. Grattan and B. T. Meggitt, *Optical Fiber Sensor Technology* (Chapman & Hall, 1995).
4. H. Y. Ryu, W. K. Lee, H. S. Moon, and H. S. Suh, Opt. Commun. **275**, 379 (2007).
5. N. Park, J. W. Dawson, K. J. Vahala, and C. Miller, Appl. Phys. Lett. **59**, 2369 (1991).
6. S. Yamashita and M. Nishihara, IEEE J. Sel. Top. Quantum Electron. **7**, 41 (2001).
7. Y. W. Song, S. A. Havstad, D. Starodubov, Y. Xie, A. E. Willner, and J. Feinberg, IEEE Photon. Technol. Lett. **13**, 1167 (2001).
8. X. He, X. Fang, C. Liao, D. N. Wang, and J. Sun, Opt. Express **17**, 21773 (2009).
9. C. S. Kim, F. N. Farokhrooz, and J. U. Kang, Opt. Lett. **29**, 1677 (2004).
10. A. P. Luo, Z. C. Luo, and W. C. Xu, Opt. Lett. **34**, 2135 (2009).
11. D. A. Smith, M. W. Maeda, J. J. Johnson, J. S. Patel, M. A. Saifi, and A. Von Lehman, Opt. Lett.**16**, 387 (1991).
12. F. Xiao, K. Alameh, and Y. T. Lee, Opt. Express **17**, 23123 (2009).
13. F. Xiao, K. Alameh, and Y. T. Lee, IEEE Photon. Technol. Lett. **23**, 182 (2011).
14. D. Sinefeld and D. M. Marom, in *Proceedings of the Conference on Lasers and Electro-Optics* (Optical Society of America, 2011), Paper CTuI5.
15. D. Sinefeld, C. R. Doerr, and D. M. Marom, Opt. Express **19**, 14532 (2011).